Journal of Materials and Engineering Structures

Research Paper

Mechanical Behaviour of Corrugated Laminates

D.J.G. Pinheiro [a], ***M.A.R. Loja*** [b, c, *], ***I.C.J. Barbosa*** [b, c], ***J. Milho*** [b, c]

[a] *OGMA, Indústria Aeronáutica de Portugal S.A., Parque Aeronáutico de Alverca, 2615-173 Alverca, Portugal*

[b] *GI-MOSM, Grupo de Investigação em Modelação e Optimização de Sistemas Multifuncionais, ISEL, IPL, Instituto Superior de Engenharia de Lisboa, Av. Conselheiro Emídio Navarro 1, 1959-007 Lisboa, Portugal*

[c] *LAETA, IDMEC, Instituto Superior Técnico, Universidade de Lisboa, Av. Rovisco Pais 1, 1049-001 Lisboa, Portugal*

ARTICLE INFO

Article history:

Received : 6 July 2018

Revised : 16 December 2018

Accepted : 18 December 2018

Keywords:

Composite materials

Corrugated panels

Finite element modelling

Free vibration analysis

Static analysis

ABSTRACT

The present research work intends to perform a wide set of structural analyses upon corrugated composite laminated panels and based on these analyses, to assess their mechanical response in correspondence to the constructive solutions, which may range from the composite materials selection to the geometrical features and other modelling parameters. To improve the mechanical performance of those panels one may consider enhancing their geometrical characteristics, their corrugation shape configuration and the materials used to build them. In this latter case, when considering materials selection, laminated composites may also constitute an important alternative. In any case it is considered necessary to assess the impact that each of these parameters may have in the static and in the free vibration behaviour of the structures, in a comprehensive and detailed way. To achieve the main objective of this research work, a comprehensive and diversified set of case studies is considered in order to characterize the influence that each of the modelling, material and geometrical parameters and characteristics may have in the mechanical response of a corrugated panel. This study allowed concluding that for the wide set of design parameters considered, the fibre orientation and corrugation parameters are the ones responsible for the majority of the significantly improved performances.

1 Introduction

Corrugated panels may constitute an important structural solution in different engineering fields. They are frequently used in sandwich structures, roofing, and many other applications in the civil, mechanical, aeronautical and naval industries. This increasing application of corrugated panels is mainly due to the high strength/weight ratio obtained with the corrugations, thus avoiding the need of using structural stiffeners and joining features that may contribute to undesirable stresses concentrations. Simultaneously, if one considers the often high stiffness and strength/weight ratios of laminates, the potential usage of these materials in corrugated panels may be a relevant solution in many engineering applications, namely when

* *Corresponding author. Tel.: +351 218 317 000 ext.1306.*
E-mail address: amelialoja@dem.isel.ipl.pt

e-ISSN: 2170-127X,

RESEARCH REVIEW of Sciences and Technologies

combined compression and torsion loads are present. In fact, nowadays, we can find fibre-reinforced composites in the production of aircraft structures, as well as in chassis of sports vehicles or even in bicycle frames, among other applications. From the literature review, it is possible to conclude that since years ago, corrugated panels were identified as potentially relevant structural elements. Formulations were performed to calculate the flexural stiffness coefficients and membrane characteristics of corrugated plates, considering different corrugations' shapes such as sinusoidal, elliptic and arc tangent ones as well as alveolar panels [1, 2]. Several analyses were performed to characterize corrugated panels. Some in terms of the effects of geometric parameters and boundary conditions on the panels' strength, where it was found that corrugations of sandwiched panel cores should be between 45 and 70 degrees, the relationship between the height of the corrugation and the thickness should be about 20, and the relationship between the length of the corrugation and the height should be between 0.5 and 0.6 [3]. Others, considering the free vibration analysis of a corrugated panel of isotropic and composite materials by discretizing the panel with triangular shear flexible elements. The element performance was tested for boundary conditions, corrugation angle and stacking sequences [4]. Also, the Galerkin-free method was used to study elastic deformation and for the dynamic assessment of corrugated reinforced plates and with simple structural reinforcements [5, 6]. The corrugated panel was treated as if it was a simple orthotropic plate (no corrugations) with different flexural properties in two perpendicular directions. Equivalent bending properties were estimated by applying constant curvature conditions to the corrugated plate. By imposing the deformation energy of the orthotropic panel and the beams, as well as the conditions of compatibility of displacements of panel and beams, the stiffness matrix of the structure was obtained and the results obtained compared with a finite element analysis commercial software to demonstrate the convergence of values. The explicit expressions to calculate the equivalent material properties of a corrugated panel were obtained by using a homogenisation-based analytical model of corrugated panels, based on a simplified geometry for a unit-cell and the stiffness properties of original sheet [7]. The bending and buckling behaviour of corrugated soft-core sandwich plates with laminated composite face sheets, when submitted to uniaxial loads was also studied using numerical solutions obtained in Ansys [8] concerning the contribution of corrugation shape, face sheet lay-up architecture, and length/thickness ratio of the plate on the bending behaviour and linear uniaxial buckling loads of the sandwich plates [9]. The dynamic analysis of corrugated panels also focus on questions regarding the equilibrium of such panels support the design in terms of a range of different corrugation patterns and support conditions in the initial stage of design [10], or the effect of the corrugations on the fundamental frequencies of the plate structures [11]. From the literature review carried out, it is possible to conclude that although the study of the mechanical response of corrugated panels is a relevant topic it hasn't so far deserved a more extended attention. The majority of the work developed, focus isotropic panels and only a few consider other type of materials. Additionally, the influence of modelling parameters is not usually considered in the studies found in related studies. It is therefore important to perform a comprehensive assessment of the mechanical response of such structures, considering a diverse range of parameters that may influence the results obtained. With the present work, this objective is addressed by developing a parametric study of material, geometrical and modelling parameters influence on the mechanical response of these structures, considering they are built from different laminated composite materials and may possess different corrugation geometrical characteristics.

2 Materials and methods

2.1 Laminated composite materials

The laminated composite panels that will be considered in the present study are made of composite materials obtained from the stacking of plies that result from the embedding of long fibre reinforced composites within an epoxy resin matrix.

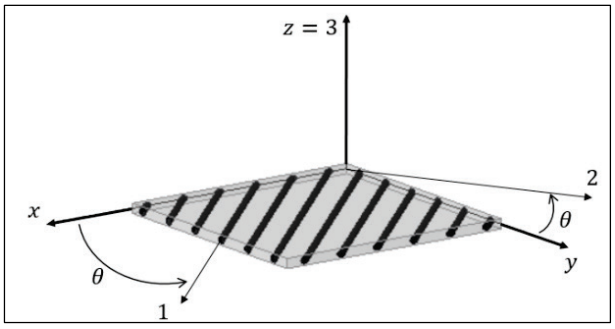

Fig. 1 –Schematic representation of a fibre reinforced composite layer

Figure 1 illustrates the orientation of the fibres within one ply and relates the coordinate system associated to the fibre orientation – the material system (123) – and the laminate coordinate system (xyz) [12]. As in a wide number of real situations, the structures can be considered as thin or moderately thin structures, it is reasonable in such conditions to assume that a plane stress condition is verified.

Accordingly, the constitutive relation for each *k* ply, under isothermal conditions, described in the laminate coordinate system can be written as:

$$\begin{Bmatrix} \sigma_{xx}^{(k)} \\ \sigma_{yy}^{(k)} \\ \tau_{xy}^{(k)} \end{Bmatrix} = \begin{bmatrix} \bar{Q}_{11}^{(k)} & \bar{Q}_{12}^{(k)} & \bar{Q}_{16}^{(k)} \\ \bar{Q}_{12}^{(k)} & \bar{Q}_{22}^{(k)} & \bar{Q}_{26}^{(k)} \\ \bar{Q}_{16}^{(k)} & \bar{Q}_{26}^{(k)} & \bar{Q}_{66}^{(k)} \end{bmatrix} \begin{Bmatrix} \varepsilon_{xx} \\ \varepsilon_{yy} \\ \gamma_{xy} \end{Bmatrix}; \begin{Bmatrix} \tau_{yz}^{(k)} \\ \tau_{zx}^{(k)} \end{Bmatrix} = \begin{bmatrix} \bar{Q}_{44}^{(k)} & \bar{Q}_{45}^{(k)} \\ \bar{Q}_{45}^{(k)} & \bar{Q}_{55}^{(k)} \end{bmatrix} \begin{Bmatrix} \gamma_{yz} \\ \gamma_{zx} \end{Bmatrix} \tag{1}$$

where the reduced transformed elastic stiffness coefficients $\bar{Q}_{ij}$ are given in the specialized literature [13, 14]. The materials used in the present work, consider three different types of fibres, namely carbon, e-glass and aramid fibres, and an epoxy resin matrix. The panels were all made from these materials, and constructively they result from the superposition of unidirectional pre-impregnated composites plies (prepregs), in perfect adhesion among each other. The properties for each of the composite material used, i.e. carbon-epoxy composite, glass-epoxy and aramid-epoxy composites, are presented in Table 1.

Table 1 - Mechanical properties of unidirectional prepregs

Prepreg properties	**Carbon-Epoxy**	**Glass-Epoxy**	**Aramid-Epoxy**
Volume fraction (V_f) [%]	66	50	60
Density (ρ) $[kg/m^3]$	1600	2000	1380
Longitudinal elasticity modulus (E_1) [GPa]	138	43	87
Transversal elasticity modulus (E_2) [GPa]	8.96	8.9	5.5
In-plane shear modulus (G_{12}) [GPa]	7.1	4.5	2.2
Poisson's ratio (ν_{12})	0.3	0.27	0.34

These properties will be used along the different case studies considered on the present work.

2.2 Corrugated panels modelling

The geometrical modelling of the corrugated panels and the corresponding finite element analyses were carried out using the finite element analyses software Ansys12 [8]. Two different commonly used cross-section profiles were analysed; namely with sinusoidal and trapezoidal cross-section.

The profile and corresponding parameters associated to the geometrical modelling of the sinusoidal corrugated panels are presented in Figure 2.

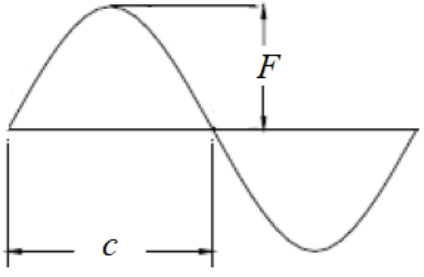

Length *L* [m]	1.8
Width *W* [m]	1.8
Thickness *h* [m]	0.018
Peak *F* [m]	0.01
Half-wavelength *c* [m]	0.1

Fig. 2–Sinusoidal corrugation and plate geometrical characteristics

Figure 3 illustrates the panel obtained with these geometrical characteristics, as well as its mesh representation for subsequent finite element analyses purposes. As one may conclude from the aspect ratio value $\left(\frac{L}{h} = \frac{W}{h} = 100 \gg 10\right)$, this plate can be considered a thin structure.

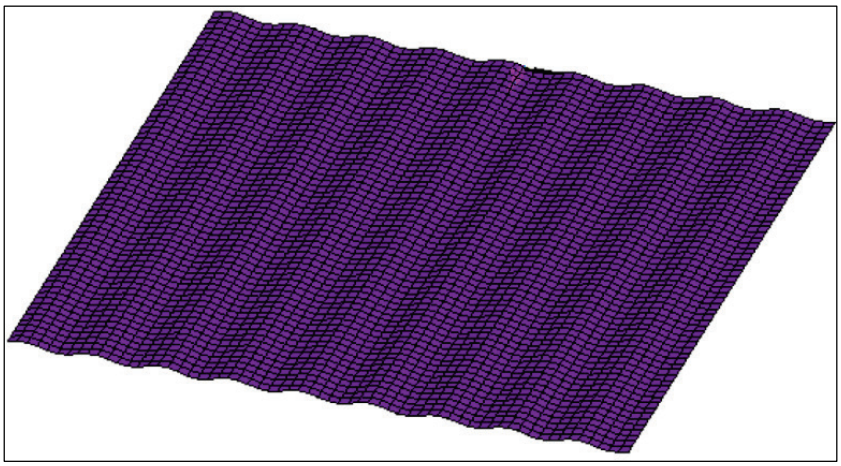

Fig. 3–Sinusoidal corrugated panel modelled in Ansys12

As mentioned, this work considers as well trapezoidal corrugations, as schematically represented in Figure 4. In this second corrugation profile, another geometrical parameter is needed for a complete characterization and subsequent analyses, the angle θ.

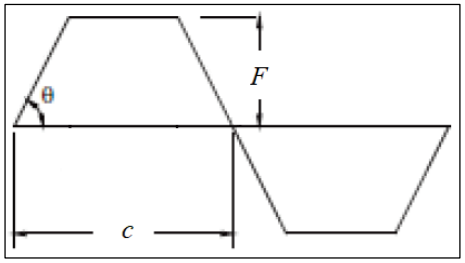

Fig. 4–Schematic representation of trapezoidal corrugation

After the parametric geometrical modelling of each type of panel, and aiming the development of finite element analysis to characterize the static and free vibrations behaviour of these panels, one has considered the use of shell elements, as they satisfy the requirements of the study considering the thin structure characteristics.

To illustrate the location of the coordinate system in the plate context, Figure 5 represents the example of a fully clamped plate, being the corrugation longitudinal direction coincident with the y direction.

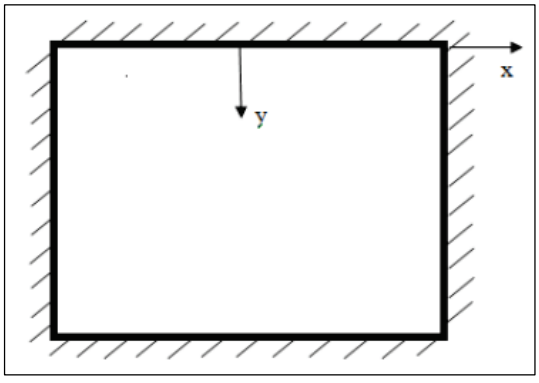

Fig. 5–Schematic representation of the coordinate system used

Concerning the boundary conditions, the panels considered on this study may be simply supported or fully clamped along their all four edges.

2.3 Verification of developed models

To perform a preliminary verification of the results obtained in the present work, one has carried out a linear static analysis of a sinusoidal corrugated panel. The panel was considered as simply supported having the material properties $E = 30\ GPa$ and $\nu = 0.3$ [5]. A uniform pressure load of 100 Pa, was applied transversally to the panel xy plane. As the panel is a thin isotropic panel, one has selected the Shell63 element, which is a four-node element with six degrees of freedom at each node, and according to Ansys [8] documentation, it is suitable for the analysis of elastic shells, and has both bending and membrane capabilities. Both in-plane and normal loads are permitted.

The discretized domain considered a mesh of (62×60) quadrilateral elements corresponding to 3843 nodes. The displacements along $x = 0.9\ m$ and $y = 0.9\ m$ are presented in Figure 6 and 7 respectively, for half-plate dimension, considering symmetry conditions. To note that in this verification case, the coordinate systems were located at a panel vertex [5, 6].

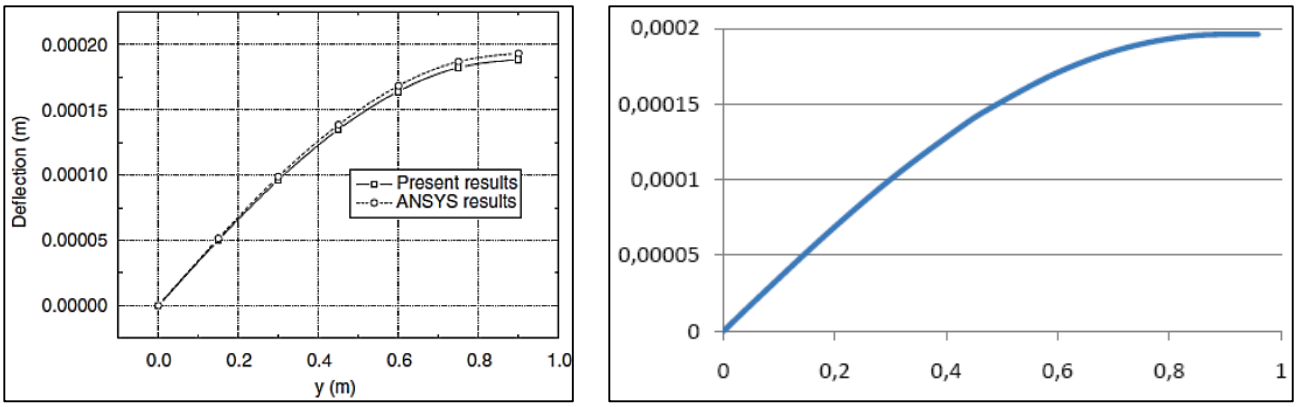

(a) (b)

Fig. 6–Deflection [m] along line $x = 0.9\ m$; (a) Ansys [5]; (b) Present

As it is possible to observe, there is a good agreement between the current model response and the solutions obtained by Ansys [5], thus allowing concluding on the present approach ability to predict the static deflection profile of the corrugated panel.

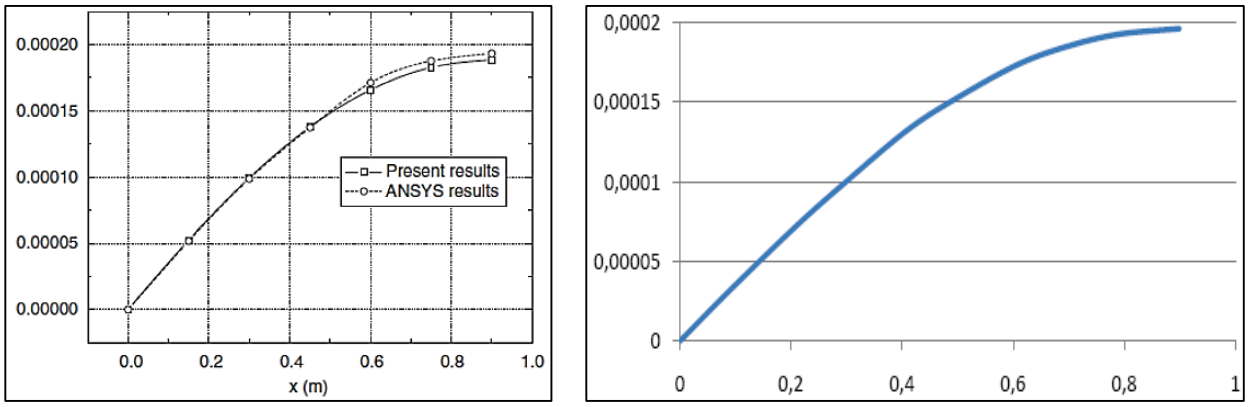

(a) (b)

Fig. 7–Deflection [m] along line $y = 0.9\ m$; (a) Ansys [5]; (b) Present

Besides the validation for the static analysis case, one has further considered another study concerning the dynamic behaviour [6].

Table 2 - Frequencies (Hz) and relative deviations (%)

Mode	Previous model [6]	Current model	Relative deviation (%)
1	23.81	23.60	-0.88
2	41.01	40.88	-0.32
3	55.26	54.59	-1.21
4	70.01	69.58	-0.61
5	70.15	69.98	-0.24
6	96.80	96.43	-0.38
7	102.65	101.32	-1.30
8	109.92	109.97	0.05
9	117.27	116.01	-1.07
10	135.13	134.75	-0.28

In this case one has used a (134×130) mesh, yielding a total of 17685 nodes. The results obtained are presented in Table 2, being the relative deviation determined as the ratio of the difference between the current model solution and the solution from reference [6] with respect to the last one, given by $Relative\ deviation(\%) = \frac{Current\ model - Ref.[6]}{Ref.[6]} \times 100$. Considering a maximum absolute deviation of 1.3% for the first six modes, a very good agreement is verified between the current model results and the ones obtained by the previous study [6].

3 Results

Considering the models good performance, several extended studies were then performed to assess the influence of the diverse parameters in the mechanical performance of the corrugated plates.

This section considers a first set of cases where the influence of the discretization of the panel and the type of shell element selected and the number of elements/nodes is analysed. After this, a second set of case studies were then considered aiming to characterize the influence of the material, geometrical and boundary conditions of the panel.

3.1 Influence of finite element models

To illustrate the influence of using different shell elements on the finite element analysis of these panels, one has considered some more often used finite elements in a static analysis case, the Shell element types 91, 99, 181 and 281. To this purpose a thin carbon-fibre composite plate with a sinusoidal corrugation profile was considered, being its thickness 0.00225 m and the fibre orientation 0º. The plate was discretized in a (74×72) mesh. The maximum deflections along the central line when a uniform transverse pressure loading of $100\ Pa$ is applied are presented in Table 3 for half the plate dimension, considering its symmetry conditions.

It can be observed that, with the exception of element Shell181, there is a fair agreement among the solutions given by the different elements. Shell181 presents a less conservative pattern, yielding higher displacement values.

Also for a free vibration analysis, and for the first ten modes, a similar conclusion is obtained as we may see in Table 4, with the Shell181 predicting in the current case lower frequency values when compared to the other shell elements. The plate was now fully clamped along its four borders and discretized in a (93×90) mesh.

Table 3 - Maximum deflection along line $x = 0\ m$ as a function of finite element type

y [m]	Deflection [m]			
	Shell91	**Shell99**	**Shell181**	**Shell281**
0	0	0	0	0
0.1	1.81e-4	1.81e-4	2.06e-4	1.81e-4
0.2	3.45e-4	3.45e-4	3.95e-4	3.45e-4
0.3	4.96e-4	4.96e-4	5.70e-4	4.97e-4
0.4	6.32e-4	6.32e-4	7.26e-4	6.32e-4
0.5	7.48e-4	7.58e-4	8.60e-4	7.48e-4
0.6	8.41e-4	8.41e-4	9.67e-4	8.42e-3
0.7	9.09e-4	9.09e-4	1.05e-3	9.10e-4
0.8	9.51e-4	9.51e-4	1.09e-3	9.52e-4
0.9	9.65e-4	9.65e-4	1.11e-3	9.66e-4

Table 4 - First modes of vibration as function of finite element type

Mode	Frequency [Hz]			
	Shell91	**Shell99**	**Shell181**	**Shell281**
1	62.12	62.20	59.73	62.10
2	64.72	64.72	62.33	64.69
3	69.21	69.21	67.01	69.19
4	75.96	75.96	73.63	75.94
5	84.79	84.79	82.52	84.77
6	96.21	96.21	94.04	96.19
7	109.99	109.99	108.05	109.98
8	127.20	127.20	125.43	127.18
9	147.00	147.00	144.73	146.99
10	149.27	149.27	145.60	149.22

Although Shell181 could be recommended for the element type to adopt as it is less expensive from the computational perspective, one has decided to further use the Shell281, due not only to its better adequacy to conform non-plane morphologies of the structures to analyse but also due to the material anisotropy associated to the composite materials used.

3.2 Influence of number of elements

In order to determine the more adequate discretization to be used, and additionally to characterize the influence of the number of elements in the discretization of the corrugated plate, one has considered the same simply supported plate of the previous case study. A similar load of 100 Pa was applied. Four different dimensions were selected for the element edges, namely 50×10^{-3}m, 40×10^{-3}m, 25×10^{-3}m and 15×10^{-3}m. These dimensions correspond to the meshes (37×36), (47×45), (74×72) and (123×120) respectively.

The deflection along $x = 0\ m,$ is presented in Table 5 for half the plate dimension, considering its symmetry conditions. As it is possible to observe in two of the cases, it is not possible to obtain results in some common specific locations as there are no nodes coinciding with those locations.

Table 5 - Deflection ($\times 10^{-4}\ m$) along line $x = 0\ m$, as a function of mesh size

y [m]	Element edge length [$\times 10^{-3}$m]			
	50	**40**	**25**	**15**
0	0	0	0	0
0.1	1.81	-	1.81	-
0.2	3.46	3.44	3.45	-
0.3	4.99	-	4.97	4.96
0.4	6.35	6.32	6.32	-
0.5	7.52	-	7.48	-
0.6	8.46	8.41	8.42	8.40
0.7	9.14	-	9.10	-
0.8	9.56	9.51	9.52	-
0.9	9.70	-	9.66	9.64

As we may see, there are small differences, less than 0.001×10^{-3}m , among the solutions for different locations, and it is also possible to observe the convergence trend of the solution, as it would be expectable. Considering these results, an edge length of 25×10^{-3}m is considered a reliable solution for static analyses purposes, in the next cases.

One has next considered a fully clamped corrugated panel, and determined the fundamental frequencies, which can be observed in Table 6.The convergence trend for this solution is perceptible from Table 6. Considering the results obtained and the associated computational cost, for subsequent analyses, a 93×90 mesh is assumed a reliable discretization for subsequent free vibration analyses.

Table 6 - Fundamental frequency Ω (Hz) as function of number of nodes

Nodes / Mesh	Ω [Hz]
100615 / (185x180)	62.12
44767 / (123x120)	62.11
25477 / (93x90)	62.10
16277 / (74x72)	62.06
11405 / (62x60)	61.99

3.3 Influence of fibre orientation angle

The influence of fibre orientation angle on the deflection of the sinusoidal corrugated plate is now considered. The same simply supported carbon-fibre plate with unidirectional stacking is submitted to a uniform transverse pressure loading of 100 Pa. The fibre orientation angle is made to vary from 0º to 90º, with 15º steps. A 0º angle means that the fibre is parallel to the x-axis of the plate.

The deflection along the line $x = 0\ m$ is characterized in Table 7 for different fibre angles.It is possible to observe the symmetry of the deflected shape along $x = 0\ m$, and its increasing trend when the orientation angle increases from 0º to 90º.

Concerning the deflection along the middle line in the y direction, the results obtained are presented in Table 8. As one may observe, the increasing trend of the deflection is maintained when the orientation angle increases, however the symmetry profile disappears in some cases.

Table 7 - Fundamental frequency Ω (Hz) as function of number of nodes

y [m]	Fibre orientation angles						
	[0°]	[15°]	[30°]	[45°]	[60°]	[75°]	[90°]
0	0	0	0	0	0	0	0
0.1	1.8	3.5	8.2	14.2	19.8	24.0	25.6
0.2	3.5	6.8	15.9	27.7	38.7	47.1	50.3
0.3	4.9	9.7	23.0	40.3	56.4	68.6	73.3
0.4	6.3	12.4	29.4	51.6	72.2	87.8	94.0
0.5	7.5	14.7	34.9	61.2	85.8	104.0	112.0
0.6	8.4	16.5	39.4	69.0	96.7	118.0	126.0
0.7	9.1	17.9	42.6	74.7	105.0	127.0	136.0
0.8	9.5	18.7	44.6	78.2	110.0	133.0	143.0
0.9	9.7	19.0	45.3	79.4	111.0	135.0	145.0
1.0	9.5	18.7	44.6	78.2	110.0	133.0	143.0
1.1	9.1	17.9	42.6	74.7	105.0	127.0	136.0
1.2	8.4	16.5	39.4	69.0	96.7	118.0	126.0
1.3	7.5	14.7	34.9	61.2	85.8	104.0	112.0
1.4	6.3	12.4	29.4	51.5	72.2	87.8	94.0
1.5	4.9	9.7	23.0	40.3	56.4	68.6	73.3
1.6	3.5	6.8	15.9	27.7	38.7	47.1	50.3
1.7	1.8	3.5	8.16	14.2	19.8	24.0	25.6
1.8	0	0	0	0	0	0	0

Table 8 - Deflection ($\times 10^{-4}\ m$) along line $y = 0.9\ m$, as function of fibre orientation

x [m]	Fibre orientation angles						
	[0°]	[15°]	[30°]	[45°]	[60°]	[75°]	[90°]
-0.9	0	0	0	0	0	0	0
-0.8	5.5	9.0	15.4	20.3	23.9	26.7	27.9
-0.7	8.3	14.8	27.7	38.2	46.0	51.8	54.2
-0.6	9.7	18.0	36.0	52.3	65.0	74.1	77.8
-0.5	9.6	18.7	40.8	63.4	81.8	94.9	100.0
-0.4	9.5	18.7	43.1	70.2	93.0	110.0	116.0
-0.3	9.7	19.1	44.5	74.7	101.0	121.0	129.0
-0.2	10.0	19.5	45.5	77.6	107.0	129.0	138.0
-0.1	9.9	19.5	45.7	79.1	110.0	134.0	143.0
0	9.7	19.0	45.3	79.4	111.0	135.0	145.0
0.1	9.4	18.7	45.0	78.7	110.0	133.0	143.0
0.2	9.7	19.0	45.0	77.3	107.0	129.0	137.0
0.3	10.0	19.5	44.9	74.8	101.0	121.0	129.0
0.4	10.0	19.5	43.6	70.3	93.0	110.0	116.0
0.5	9.6	18.6	40.7	63.3	81.6	94.8	100.0
0.6	9.0	17.0	35.2	52.0	64.8	74.0	77.7
0.7	7.8	14.1	27.1	37.9	45.9	51.8	54.2
0.8	5.5	8.9	15.2	20.2	23.9	26.8	28.0
0.9	0	0	0	0	0	0	0

It is possible to perceive that for lower fibre angles, the deflection is not symmetric along the line y = 0.9 m, but this effect dissipates as the fibre angle increases.

Table 9 - Natural frequencies (Hz) as function of fibre orientation angles

Mode	Fibre orientation angles						
	[0°]	[15°]	[30°]	[45°]	[60°]	[75°]	[90°]
1	62.11	51.85	34.39	25.64	21.60	19.82	19.33
2	64.70	54.12	36.89	29.22	26.76	26.45	26.57
3	69.19	58.29	41.64	36.32	37.27	40.10	41.55
4	75.94	64.46	48.73	47.05	52.81	51.41	49.74
5	84.77	73.17	58.83	61.65	57.15	57.02	55.34
6	96.19	84.72	71.95	69.35	62.43	59.90	63.50
7	109.98	99.29	88.22	74.17	72.53	69.04	67.54
8	127.18	117.41	94.83	79.26	73.24	83.17	86.83
9	146.99	138.86	99.05	83.48	88.71	89.98	91.89
10	149.22	139.34	105.77	94.25	96.77	98.50	95.11

When free vibrations are studied as presented in Table 9, it is observed that the fundamental frequencies values reveal the expected behaviour when related to the deflection profiles previously identified. As the orientation angle increases the fundamental frequency decreases.

When one considers higher vibration modes, we may observe a different response pattern, which is illustrated in the Figure 8.

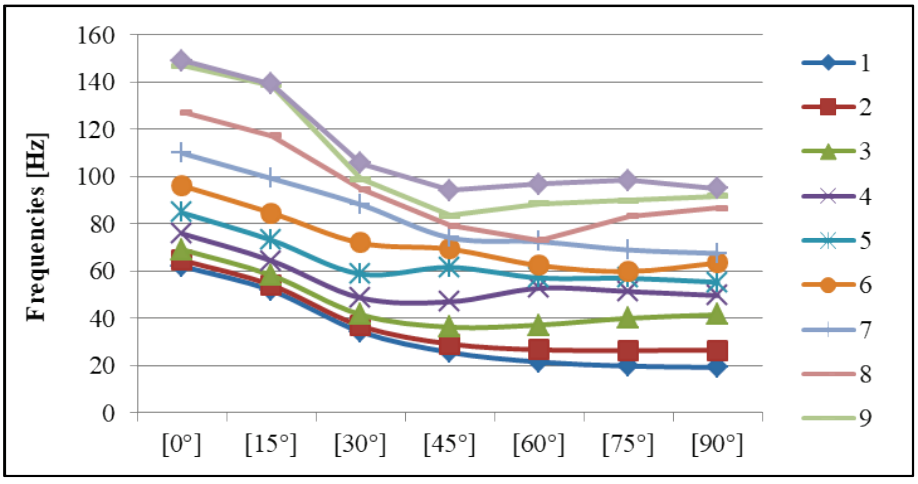

Fig. 8–Natural frequencies as function of fibre orientation for the first ten modes of vibration

As depicted in Figure 8, the first two natural frequencies follow a monotonic decreasing trend when the orientation angle increases, while the remaining frequencies inflect this trend for different orientation angles.

3.4 Influence of the number of layers and stacking sequence

In this case study we consider for the same thin plate, the influence of the number of layers, three or nine, and its stacking. To this purpose, in a first analysis one compares two cross-ply laminates with the same total thickness but with a different number of layers. The corresponding deflections along $x = 0\ m$ are presented in Table 10, for half the plate dimension, considering its symmetry conditions.

Table 10 - Deflection along line $x = 0\ m$, ($\times 10^{-4}\ m$), as a function of the stacking sequence

y [m]	Stacking Sequence	
	[90/0/90]	$[[90/0]_8/90]$
0	0	0
0.1	4.8	3.7
0.2	9.3	7.2
0.3	13.6	10.4
0.4	17.4	13.3
0.5	20.6	15.8
0.6	23.3	17.8
0.7	25.2	19.3
0.8	26.4	20.2
0.9	26.8	20.5

As we may conclude, the laminate with a higher number of layers, presents lower deflections and therefore a less flexible behaviour which is an expected situation, as its stiffness becomes greater when compared to the laminate with three layers. The elastic line of the three-layered cross-ply configuration is therefore more pronounced.

Considering now different stacking sequences involving the 45º, -45º and 0º angles, and also different number of layers, we obtain the deflection along $x = 0\ m$ as presented in Table 11.From this table one concludes that again the three-layered configuration yield a greater deflection profile when comparing to the nine-layered composite. This is valid for both basis configurations [45º/0º/45º] and [45º/0º/-45º].It is also possible to conclude that anti-symmetric configuration [45º/0º/-45º] provide a stiffer response when compared to the symmetric [45º/0º/45º]. However, when considering the laminates with nine layers, the $[45º/0º/45º]_3$ presents a stiffer behaviour.

Table 11 - Deflection along line $x = 0\ m$, ($\times 10^{-4}\ m$), as a function of the stacking sequence

y [m]	Stacking Sequence			
	[45/0/45]	[45/0/-45]	$[[45/0]_8/45]$	$[45/0/-45]_3$
0	0	0	0	0
0.1	4.1	3.6	3.3	3.6
0.2	7.9	7.1	6.3	7.1
0.3	11.4	10.4	9.2	10.4
0.4	14.6	13.4	11.7	13.3
0.5	17.4	15.9	13.9	15.8
0.6	19.6	17.9	15.7	17.8
0.7	21.2	19.4	17.0	19.2
0.8	22.1	20.4	17.8	20.1
0.9	22.5	20.7	18.0	20.5
1.0	22.1	20.4	17.8	20.2
1.1	21.2	19.5	17.0	19.3
1.2	19.5	18.0	15.7	17.8
1.3	17.3	16.0	13.9	15.8
1.4	14.6	13.5	11.7	13.3
1.5	11.4	10.6	9.2	10.4
1.6	7.9	7.3	6.3	7.2
1.7	4.1	3.8	3.3	3.7
1.8	0	0	0	0

In a more global interpretation, it is possible to conclude that the stiffening effect arising from the number of layers increase is clearly more visible in the [45º/0º/45º] and $[45º/0º/45º]_3$ cases. The stiffening gain in the other case is minor.

The influence of these parameters was also assessed in the free vibrations analysis presented in Table 12. Again, for the two first cross-ply laminates, it is possible to see that for the nine-layers composite $[[90/0]_8/90]$ where we predicted a less flexible behaviour we find a greater value for the fundamental frequency. Concerning to the higher vibration modes, one finds that for some of the modes, the three-layered composite presents higher frequency values.

Table 12 - Natural frequencies (Hz) as a function of the stacking sequence

Vibration Mode	Stacking sequence	
	[90/0/90]	$[[90/0]_8/90]$
1	41.98	46.58
2	47.13	50.84
3	58.86	60.26
4	77.69	75.38
5	104.14	97.21
6	107.39	118.15
7	113.34	123.78
8	125.07	125.22
9	137.47	134.37
10	142.85	150.25

Considering now the basis configurations [45º/0º/45º] and [45º/0º/-45º] presented in Table 13, one concludes that the symmetric stacking predicts a lower fundamental frequency.

Table 13 - Natural frequencies (Hz) as a function of the stacking sequence

Vibration Mode	Stacking sequence			
	[45/0/45]	[45/0/-45]	$[[45/0]_8$ /(45]	$[45/0/-45]_3$
1	45.63	46.81	50.03	47.77
2	49.20	49.98	53.37	51.30
3	56.16	55.85	59.74	58.02
4	66.63	64.43	69.19	67.97
5	81.60	76.57	82.71	82.18
6	100.93	92.42	100.33	100.60
7	120.59	112.21	122.21	123.71
8	124.77	124.66	131.21	128.45
9	126.86	131.20	137.04	135.26
10	136.98	136.72	146.68	146.93

In what concerns to the higher modes of vibration, there is no observable specific trend for different stacking and fibre orientation, which is highly dependent on each vibration mode as we may observe in Figure 9.

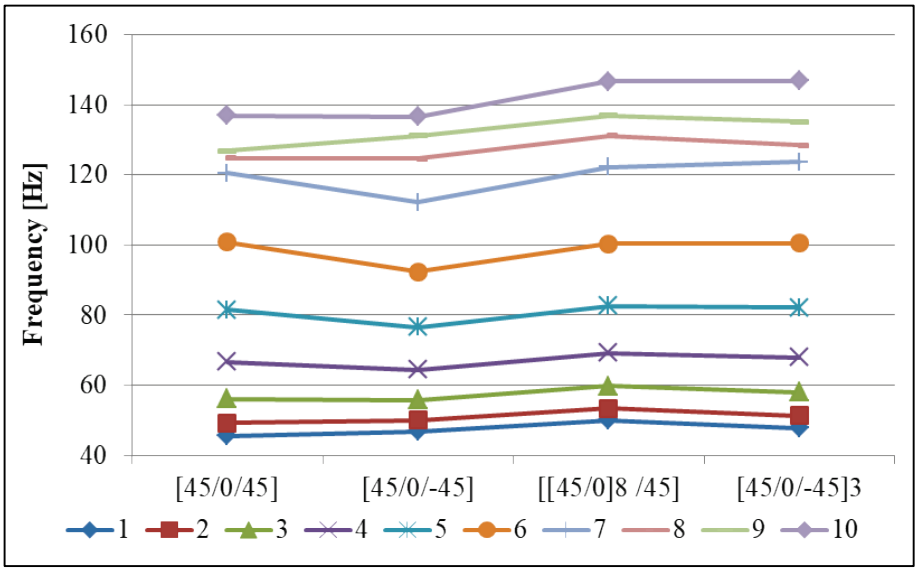

Fig. 9–Natural frequencies as function of stacking and fibre orientation

In the nine-layered composites [[45º/0º]$_8$/45º] and [45º/0º/-45º]$_3$, the higher fundamental frequency is exhibited by the [[45º/0º]$_8$/45º] composite panel.

3.5 Influence of material properties

The influence of the material properties is considered in the present case study, by assuming three different prepregs, with properties given in Table 1.

The sinusoidal corrugated plates used in this case study are similar to the ones in previous case studies. In the static analysis, the simply-supported plate has a thickness of 0.00225 m and it is submitted to a uniform pressure loading of 100 Pa. The fibre orientation angle is 0º. The deflection profiles of the three plates along the line $x = 0\ m$ are given in Table 14. It can be seen that the carbon-epoxy composite provided a stiffer panel thus leading to a more conservative deflection profile. The glass-epoxy composite was responsible for the more flexible panel.

Table 14 - Deflection ($\times 10^{-4}\ m$) along line $x = 0\ m$ as a function of the material properties

y [m]	Reinforcement Fibre		
	Carbon	Glass	Aramid
0	0	0	0
0.1	1.8	5.5	3.1
0.2	3.5	10.6	5.8
0.3	5.0	15.3	8.4
0.4	6.3	19.6	10.7
0.5	7.5	23.3	12.6
0.6	8.4	26.2	14.2
0.7	9.1	28.3	15.3
0.8	9.5	29.7	16.0
0.9	9.7	30.1	16.2

In a free vibration perspective and again maintaining the characteristics used in this type of analysis, it is possible to conclude from the corresponding results in Table 15 that the higher fundamental frequency predicted corresponds to the carbon-epoxy composite plate.

Table 15 - Natural frequencies (Hz) as a function of the material properties

Vibration Mode	Natural frequencies [Hz]		
	Carbon	Glass	Aramid
1	62.10	47.63	33.23
2	64.70	49.33	35.03
3	69.19	52.31	38.36
4	75.94	56.99	43.25
5	84.77	63.03	50.15
6	96.19	70.98	59.19
7	109.98	80.64	70.42
8	127.18	92.72	84.18
9	146.99	106.70	84.49
10	149.22	108.02	87.71

Similarly, the lower fundamental frequency is predicted for the glass-epoxy corrugated panel. As expected for higher vibration modes, the natural frequencies increase in a similar way for the different materials.

3.6 Influence of the boundary conditions

The influence of boundary conditions was studied and different boundary conditions were explored; namely, simply supported (SSSS) and clamped (CCCC) along their four edges. The plates' remaining parameters used for the static and free vibration analysis are similar to the ones used in previous case studies. Thus the results for the static and free vibration analyses are presented in Tables 16 and 17.

The deflection results in Table 16 are presented for half the plate dimension, considering its symmetry conditions. As expected the deflection profiles decrease as the stiffening effect of the boundary conditions become higher.

Table 16 - Deflection [m] along line $x = 0\ m$ as a function of boundary conditions

y [m]	Boundaries	
	SSSS	CCCC
0	0	0
0.1	1.81E-04	1.93E-05
0.2	3.45E-04	5.06E-05
0.3	4.97E-04	8.67E-05
0.4	6.32E-04	1.24E-04
0.5	7.48E-04	1.60E-04
0.6	8.42E-04	1.91E-04
0.7	9.10E-04	2.15E-04
0.8	9.52E-04	2.30E-04
0.9	9.66E-04	2.35E-04

Concerning to the free vibration analysis, the results considering these boundary conditions are presented in Table 17.

Table 17 - Natural frequency (Hz) as a function of boundary conditions

Vibration Mode	Boundaries	
	SSSS	CCCC
1	30.35	62.10
2	31.82	64.70
3	34.54	69.19
4	38.81	75.94
5	45.15	84.77
6	53.52	96.19

From Table 17, it is possible to confirm that the fully clamped panel shows the higher fundamental frequency, while the less stiff boundary conditions reveal a lower fundamental frequency.

3.7 Influence of the corrugation geometry

Regarding the geometry of the corrugation profile, one studies the sinusoidal corrugation panels analysed in previous case studies. The profile of the corrugation was modified by altering the peak (F) and the half-wavelength (c) as presented in Figure 2. The results obtained for the deflection profile of the simply supported panel are presented in Table 18 for half the plate dimension, considering its symmetry conditions.

Table 18 - Deflection ($\times 10^{-4}\ m$) along line $x = 0\ m$ as a function of corrugation geometry

y [m]	Corrugation parameters					
	c=0.1m & F=0.01m	c=0.1m & F=0.02m	c=0.1m & F=0.03m	c=0.2m & F=0.01m	c=0.2m & F=0.02m	c=0.2m & F=0.03m
0	0	0	0	0	0	0
0.1	1.81	0.46	0.22	2.72	0.89	0.52
0.2	3.45	0.86	0.40	4.90	1.52	0.85
0.3	4.97	1.23	0.55	6.72	2.01	1.09
0.4	6.32	1.56	0.70	8.29	2.42	1.29
0.5	7.48	1.85	0.82	9.62	2.77	1.45
0.6	8.42	2.07	0.91	10.7	3.05	1.58
0.7	9.10	2.24	0.99	11.5	3.25	1.68
0.8	9.52	2.34	1.03	11.9	3.37	1.73
0.9	9.66	2.37	1.04	12.1	3.41	1.75

From Table 18, one can observe that when the peak of the sinusoid increases, while the half-wavelength remains unaltered, the deflection curve decreases, yielding lower deflection maximum values. Conversely, when we consider the increase of the half-wavelength for the same peak, we observe an increase of the deflection.

It is also possible to see from Figure 10 that, for the values considered, altering the peak value has a minor impact when compared to the effect of altering the half-wavelength.

A trapezoidal profile was then considered, as mentioned in Figure 4, where an additional parameter, the angle θ, is introduced and studied.

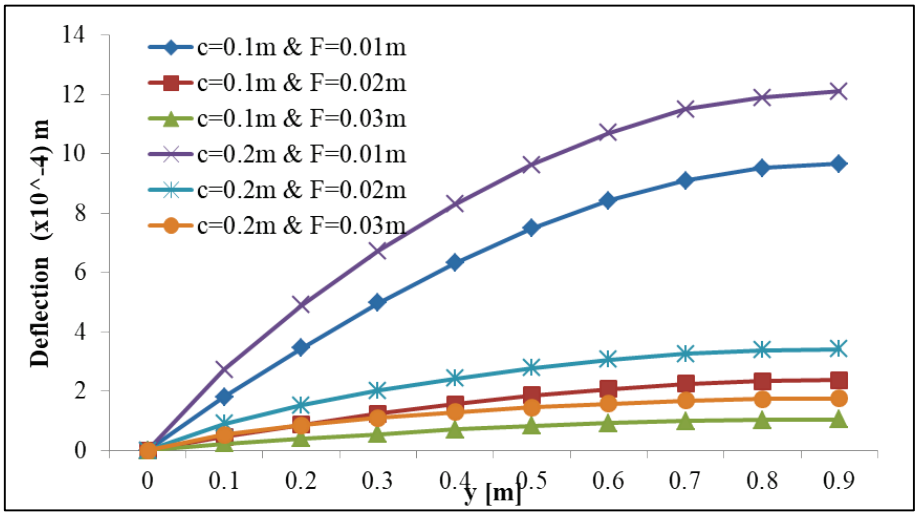

Fig. 10–Deflection ($\times 10^{-4}$ m) along line $x = 0$ m as a function of corrugation geometry

By considering now some examples of the angle θ and comparing the results obtained in the corresponding analyses, we obtain the deflection profile along the line $x = 0\,m$, presented in Table 19 for half the plate dimension, considering its symmetry conditions.

Table 19 - Deflection ($\times 10^{-4}$ m) along line $x = 0$ m as a function of type of corrugation geometry

y [m]	Corrugations			
	Sinusoidal	Trapezoidal 30º	Trapezoidal 45º	Trapezoidal 60º
0	0	0	0	0
0.1	1.81	1.11	1.01	0.96
0.2	3.45	2.13	1.95	1.86
0.3	4.97	3.08	2.81	2.70
0.4	6.32	3.93	3.59	3.44
0.5	7.48	4.65	4.25	4.08
0.6	8.42	5.24	4.78	4.59
0.7	9.10	5.66	5.17	4.96
0.8	9.52	5.92	5.41	5.19
0.9	9.66	6.01	5.49	5.26

As one may observe from Table 19, the considered trapezoidal profiles perform better than the sinusoidal one, as the deflection profiles are minor. Within these trapezoidal configurations we also observe that a higher angle provides a stiffer panel.

Considering now the deflection profiles along the line $y = 0.9\,m$, the deflections of the different corrugated panels are presented in Table 20.

In this case, we may observe again that the trapezoidal corrugations increase the stiffness of the panels, thus decreasing their deflections. The lower deflection values correspond to the higher corrugation angle.

According to the trend already identified in the case of the sinusoidal corrugation, it is possible to observe that when we consider the deflection at the middle line $y = 0.9\,m$, the deflected shape is not symmetric.

Table 20 - Deflection ($\times 10^{-4}\ m$) along line y = 0.9 m as a function of type of corrugation geometry

x [m]	Corrugations			
	Sinusoidal	Trapezoidal	Trapezoidal	Trapezoidal
-0.9	0	0	0	0
-0.8	5.49	3.68	3.45	3.18
-0.7	8.25	5.09	4.76	4.41
-0.6	9.66	5.83	5.38	5.09
-0.5	9.62	5.98	5.47	5.17
-0.4	9.45	6.02	5.47	5.21
-0.3	9.68	6.00	5.49	5.19
-0.2	10.00	6.00	5.46	5.22
-0.1	9.93	5.99	5.45	5.22
0.0	9.66	6.01	5.49	5.26
0.1	9.40	5.99	5.54	5.25
0.2	9.67	6.00	5.55	5.20
0.3	10.0	6.00	5.53	5.19
0.4	10.0	6.02	5.48	5.20
0.5	9.61	5.98	5.47	5.22
0.6	8.96	5.83	5.38	5.14
0.7	7.79	5.09	4.66	4.48
0.8	5.46	3.68	3.45	3.51
0.9	0	0	0	0

The corresponding free vibration analysis yielded the results presented in Table 21.

Table 21 - Fundamental frequency Ω (Hz) as function of the corrugation geometry

Geometry	Ω [Hz]
c=0.1m & F=0.01m	62.10
c=0.1m & F=0.02m	118.93
c=0.1m & F=0.03m	165.40
c=0.2m & F=0.01m	47.15
c=0.2m & F=0.02m	62.22
c=0.2m & F=0.03m	61.73

From this table, we may conclude that when the peak increases, the fundamental frequency also increases. Augmenting the half-wavelength for the same peak, produces a decreasing effect in the fundamental frequency.

Again, when comparing the previous set of trapezoidal panels and the sinusoidal one as presented in Table 22, we conclude that this last possesses a lower fundamental frequency. Also in the case of the trapezoidal corrugations, we observe that to a higher angle corresponds a higher fundamental frequency.

However when considering higher order modes, namely after the fifth mode, this trend doesn't hold.

Table 22 - Frequencies (Hz) as a function of the type of corrugation geometry

Vibration Mode	Corrugation			
	Sinusoidal	Trapezoidal 30º	Trapezoidal 45º	Trapezoidal 60º
1	62.10	78.15	79.93	80.83
2	64.70	81.06	82.61	83.40
3	69.19	86.00	87.17	87.55
4	75.94	93.11	93.73	94.04
5	84.77	102.68	103.58	102.48
6	96.19	114.71	116.17	113.36
7	109.98	129.19	130.49	126.20
8	127.18	146.46	148.17	142.76
9	146.99	166.09	169.13	161.17
10	149.22	187.57	190.43	181.65

Corrugated composite structures may constitute important solutions where enhanced mechanical performance is required guaranteeing high stiffness to weight and strength to weight ratios.

This work developed a set of parametric studies ranging from the material and geometrical parameters to other related to the modelling of the panel. To this purpose linear static and free vibration analyses were performed in order to characterize the influence of such parameters on the panel response.

From the parametric studies developed it is possible to conclude that several different parameters, such as for example, fibre orientation and corrugation parameters can be responsible for significant improved performances. To illustrate this one may refer that by selecting the more adequate fibre orientation, it was possible to reduce the maximum deflection of a sinusoidal corrugated panel about fifteen times when compared to the more unfavourable fibre orientation situation. From the materials analysed it was also possible to conclude that the maximum deflection of the stiffer panel is less than one third of the more flexible one, while the fundamental frequency almost doubled. Corrugations geometry is a relevant aspect in this context. According to the trapezoidal geometries analysed it was possible to obtain deflections more than eleven times lower. Associated to this, a frequency almost four times higher was also obtained.

The results presented and discussed, allow concluding that these structures have a great versatility and potential to be adapted to different applications' requisites, and therefore suitable to be used in conjunction with optimization procedures for finding specific optimal constructive design solutions.

4 Conclusion

Corrugated composite structures may constitute important solutions where enhanced mechanical performance is required guaranteeing high stiffness to weight and strength to weight ratios.

This work developed a set of parametric studies ranging from the material and geometrical parameters to other related to the modelling of the panel. To this purpose linear static and free vibration analyses were performed in order to characterize the influence of such parameters on the panel response.

From the parametric studies developed it is possible to conclude that several different parameters, such as for example, fibre orientation and corrugation parameters can be responsible for significant improved performances. One may refer that by selecting the more adequate fibre orientation, it was possible to reduce the maximum deflection of a sinusoidal corrugated panel about fifteen times when compared to the more unfavourable fibre orientation situation. From the materials analysed it was also possible to conclude that the maximum deflection of the stiffer panel is less than one third of the more flexible one, while the fundamental frequency almost doubled. Corrugations geometry is a relevant aspect in this context. According to

the trapezoidal geometries analysed it was possible to obtain deflections more than eleven times lower. Associated to this, a frequency almost four times higher was also obtained.

The results presented and discussed allow concluding that these structures have a great versatility and potential to be adapted to different applications' requisites, and therefore suitable to be used in conjunction with optimization procedures for finding specific optimal constructive design solutions.

Acknowledgements

The authors wish to thank the support of Project LAETA-UID/EMS/50022/2013.

REFERENCES

[1]- S. Luo, J.C. Suhling, J.M. Considine, T. L. Laufenberg, The bending stiffness of corrugated board. Mech. Cellulosic Mater. 36 (1992) 15-26.

[2]- N. Buannic, P. Cartraud, T. Quesnel, Homogenization of Corrugated Core Sandwich Panels. Compos. Struct. 59(3) (2003) 298–311. doi:10.1016/S0263-8223(02)00246-5

[3]- W.S. Chang, E. Ventsel, T. Krauthammer, J. John, Bending behaviour of corrugated-core sandwich plates. Compos. Struct. 70(1) (2005) 81–89. doi:10.1016/j.compstruct.2004.08.014

[4]- S. Haldar, A.H. Sheikh, Free vibration analysis of isotropic and composite folded plates using a shear flexible element. Finite Elem. Anal. Des. 42(3) (2005) 208–226. doi:10.1016/j.finel.2005.06.003

[5]- L.X. Peng, K.M. Liew, L. Kitipornchai, Analysis of stiffened corrugated plates based on the FSDT via the mesh-free method. Int. J. Mech. Sci. 49(3) (2007) 364-378. doi:10.1016/j.ijmecsci.2006.08.018

[6]- K.M. Liew, L.X. Peng, S. Kitipornchai, Vibration Analysis of Corrugated Reissner–Mindlin Plates Using a Mesh-Free Galerkin Method. Int. J. Mech. Sci. 51(9-10) (2009) 642-652. doi:10.1016/j.ijmecsci.2009.06.005

[7]- Y. Xia, M.I. Friswell, E.I.S. Flores, Equivalent models of corrugated panels. Int. J. Solids Struct. 49 (2012) 1453–1462. doi:10.1016/j.ijsolstr.2012.02.023

[8]- Ansys Inc., Documentation for Ansys. https://www.ansys.com/ (Last accessed 20 March 2018)

[9]- M.M. Kheirikhah,V. Babaghasabha, Bending and buckling analysis of corrugated composite sandwich plates. J. Braz. Soc. Mech. Sci. 38(8) (2016) 2571-2588. doi:10.1007/s40430-016-0498-6

[10]- S. Malek, C. Williams, The Equilibrium of Corrugated Plates and Shells. Nexus Netw. J. 19(3) (2017) 619-627. doi:10.1007/s00004-017-0347-7

[11]- N. Alshabatat, Design of Corrugated Plates for Optimal Fundamental Frequency. Adv. Acoust. Vib. 2016 (2016) 1-9. doi:10.1155/2016/4290247

[12]- J.N. Reddy, Mechanics of Laminated Composite Plates, Theory and Analysis. CRC Press, First Edition, 1996.

[13]- M.A.R. Loja, J.I. Barbosa, C.M. Mota Soares, Analysis of Sandwich Beam Structures Using Kriging Based Higher Order Models. Compos. Struct. 119 (2015) 99-106. doi:10.1016/j.compstruct.2014.08.019

[14]- M.A.R. Loja, J.I. Barbosa, C.M. Mota Soares, Dynamic Behaviour of Soft Core Sandwich Structures using Kriging-Based Layerwise Models. Compos. Struct. 134 (2015) 883-894. doi:10.1016/j.compstruct.2015